ELSEVIER

Solid State Ionics 8024 (2001) xxx

SOLID STATE IONICS

www.elsevier.com/locate/ssi

Preparation and reactivity of Rh nanoparticles on $TiO_2(110)$-(1×2) surface

András Berkó, János Szökő, Frigyes Solymosi *

Reaction Kinetics Research Group of the Hungarian Academy of Sciences, Institute of Solid State and Radiochemistry, University of Szeged, P.O. Box 168, H-6701, Szeged, Hungary

Abstract

Arrays of Rh nanoparticles with independently controlled sizes and average distances were prepared by exploiting the surface temperature-dependent kinetics of the Rh adatoms and nanocluster migration processes on $TiO_2(110)$-(1×2) surface. The supported Rh nanoparticles fabricated in this way exhibit a very narrow size distribution. The characteristic particle diameter can be varied in the range of 2–20 nm with a desired interparticle distance tunable between 5 and 100 nm. The distribution and the morphology of the nanoparticles were characterized by scanning tunneling microscopy. The advantage of this method in comparison with lithography techniques is its relative simplicity and the possibility of the preparation of metal particles in the typical "catalytic regime". The model catalysts so produced are applicable in the study of size-dependent reactivity of the nanoparticles (gas-induced disruption, agglomeration, encapsulation, catalytic activity). It is also suggested that the tailored particle arrays can serve as templates for further nanostructural fabrication. © 2001 Published by Elsevier Science B.V.

Keywords: Tailored growing of nanoparticle arrays; Rhodium grown on $TiO_2(110)$-(1×2) surface; Scanning tunneling microscopy (STM); Disruption and agglomeration of nanoparticles; Dissociation of CO; Spillover of carbon

1. Introduction

Several methods have been recently developed which are capable of producing two-dimensional model catalysts (2DMC) with a very narrow particle-size distribution [1–11]. By the application of the atom probe techniques, as for example the scanning tunneling microscopy, it became recently possible to check rigorously the particle size of the 2DMC materials. Most of these preparation methods, however, usually suffer from irregular spatial distribution, low surface density of the clusters or some carbon contaminations, therefore they are inadequate for application in catalysis (or cannot fulfil all the requirements, i.e. uniform size, regular spatial distribution and sufficient numbers of metal clusters). In a recent paper, a new method was presented for the preparation of Ir nanoparticle arrays on $TiO_2(110)$-(1×2) surface [12]. The method consists of two steps: (i) vapor deposition of the metal in predetermined concentration (a few percents of monolayer) onto the support at 300 K followed by post-annealing at 1100 K; (ii) further evaporation of the metal at 1100 K onto this surface for growing the crystallites formed in the first step. The advantage of this method in comparison with lithography techniques is its relative simplicity and the potential for preparation of metal particles in the range of 1.5–20 nm.

* Corresponding author. Fax: +36-62-424-997.
E-mail address: frigyes.solymosi@chem.u-szeged.hu (F. Solymosi).

0167-2738/01/$ - see front matter © 2001 Published by Elsevier Science B.V.
PII: S0167-2738(01)00845-1

In this work, we describe how the above-mentioned method can be applied to produce well-separated Rh particles in the range of 2–3 nm up to 20–50 nm with roughly uniform sizes and controlled spatial distribution. This method is based on our recent finding that there is a great difference in the diffusion coefficient of Rh adatoms and 1–2 nm Rh nanocrystallites on oxidic supports [13–15]. Several examples are described where particle arrays that were fabricated so can be applied for further studies of gas + surface interaction. Some STM results are also presented for the thermal-induced diffusion of carbon clusters formed in the dissociation of CO.

2. Experimental

The experiments were carried out in a UHV chamber equipped with a three-grid AES-LEED analyzer and a commercial STM head purchased from WA Technology. The noble metal ultrathin layer was deposited by ohmically heated Rh filament. During the dosing, the distance between the metal source and the sample was approximately 20 mm. The rate of the deposition was controlled by adjusting the current flowing through the Rh filament. The amount and the purity of the epitaxial Rh layer on the titania were checked by AES spectroscopy. The surface concentration of the deposited metal is given in monolayer equivalent (ML), which corresponds to 1.6×10^{15} Rh atoms/cm^2. The calculation of this value based on AES and STM measurements has been described in detail earlier [13,16].

The polished TiO_2(110) single crystal sample was purchased from Crystal Tec. Without any further treatment in air, it was clipped with a Ta plate on a transferable sample holder and moved into the chamber. The sample was heated by a W filament positioned just below the Ta plate carrying the probe. By this arrangement it was possible to achieve a surface temperature of 1100 K measured by a thin chromel–alumel thermocouple forced to the edge of the sample. The cleaning procedure of the TiO_2 was outlined in our previous papers [13,17]. Highly ordered 1×2 reconstructed terraces could be obtained only after annealing at 1100 K in UHV. The characteristic morphology of TiO_2(110)-(1×2) was recently discussed in detail by several papers [17–22].

3. Results and discussion

3.1. Preparation of Rh nanoparticles of controlled size and neighbor distance

The tailored growing of Rh particles was started by exposing the clean TiO_2(110)-(1×2) surface to Rh of a few percent of a monolayer (lower than 10%) at room temperature and annealing at 1100 K in vacuum (UHV) for several minutes. This first part of the preparation is called "seeding". It is worth mentioning that, in an earlier paper, it was proved that this treatment results in Rh nanoparticles with a surface concentration linearly proportional to the amount of Rh deposited on the TiO_2(110)-(1×2) surface. Fig. 1(a,e) shows the surface morphology after exposing the clean oxide surface to 0.005 and 0.20 ML Rh at 300 K with a subsequent annealing in UHV for 10 min at 1100 K. The STM images indicate that in these cases, an average of one and seven nanoparticles are present in a region of 100×100 nm. The Rh nanocrystallites so produced possess a hexagonal shape of 3-nm diameter with 3–5 atomic layer thick plates with (111) plane parallel to the surface of the support [13]. In the second part of the preparation ("growing"), the seeded samples were exposed sequentially to further amounts of Rh at 1100 K (Fig. 1(b–d) and (f–h)). In this way, the size of the existing Rh nanoparticles gradually increased but they remained uniform for the different coverages. At about 1 ML of post-deposited Rh, the size of the metal nanoparticles attained a value of 12–18 nm. As Fig. 1(i–l) shows, the size distribution increases with the average size of the particles to a small degree. However, an important feature is that the average distance between the Rh particles remained unaltered. Although the average size and the number of Rh nanoparticles can be conveniently controlled in this way, at least two forms of Rh crystallites can be distinguished. Quasi-isotropic hexagonal crystals oriented by one side in the crystallographic direction of [001] and particles of strongly elongated shape also oriented in this direction (Fig. 1h). The quality of the size distribution of the grown particles can be seen from the histogram calculated for the samples of higher particle density

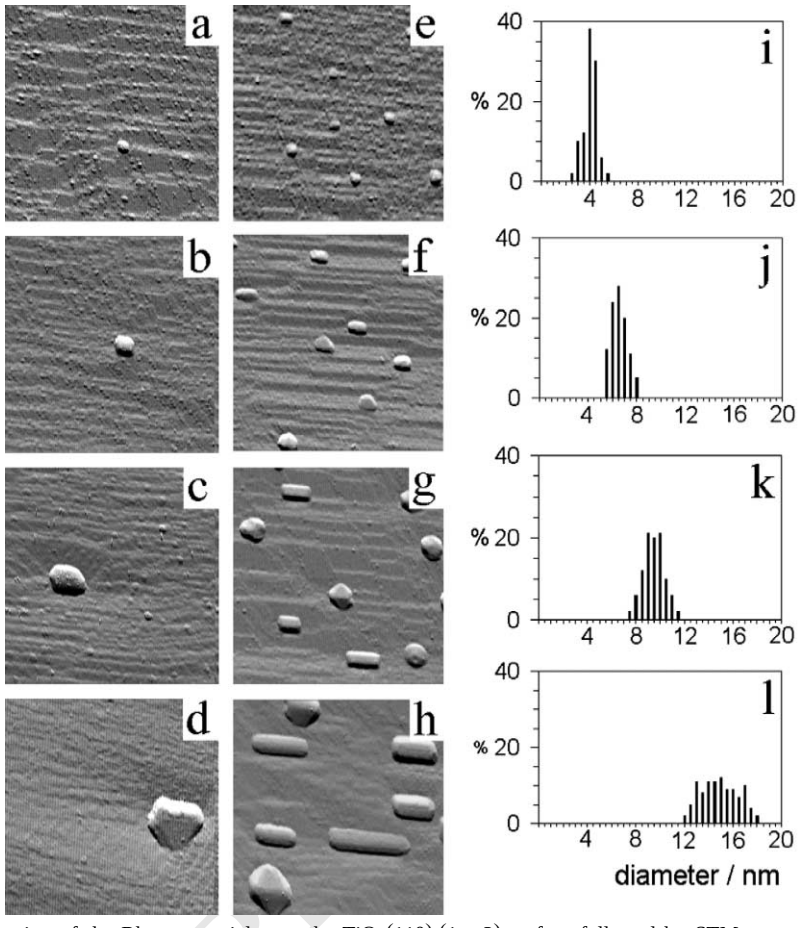

Fig. 1. Seeding and growing of the Rh nanoparticles on the $TiO_2(110)$-(1×2) surface followed by STM measurements. (a and e) The morphology after evaporation of 0.05 and 0.20 ML of Rh at 300 K and annealing at 1100 K in UHV for 10 min, respectively. (b–d and f–h) Growing of the seeds by further evaporation of Rh at 1100 K. (i–l) The size distribution of the fabricated Rh crystallites in the procedure (e–h). The size of the STM images: 100×100 nm.

(Fig. 1(i–l)). As these figures show, the average diameter gradually shifts from 3 to 15 nm; the standard deviation does not exceed 20–30%. By comparing the particle arrays to those produced with other methods, we can conclude that the monodispersity of the particles is rather good in the present case.

3.2. Adsorption-induced disruption of Rh nanoparticles

Previous studies showed that the adsorption of CO on Rh crystallites caused its disruption to smaller units and finally to isolated Rh atoms [23–28]. STM pictures presented in Fig. 2 demonstrate that this process sensitively depends on the size of Rh clusters. Rh nanoparticles of 1–2 nm readily disrupt (Fig. 2a,b), whereas particles of 10–12 nm are practically resistant towards CO (Fig. 2c,d). A somewhat more complicated size dependence was observed in the dissociation of CO on Rh nanoparticles supported on alumina by Frank et al. [29]. In this case, the probability of CO dissociation goes through a maximum for aggregates containing 1000 atoms, which belong approximately to the average particle size of 2–3 nm. It is worth mentioning that these latter results were obtained in low-pressure adsorption experiments.

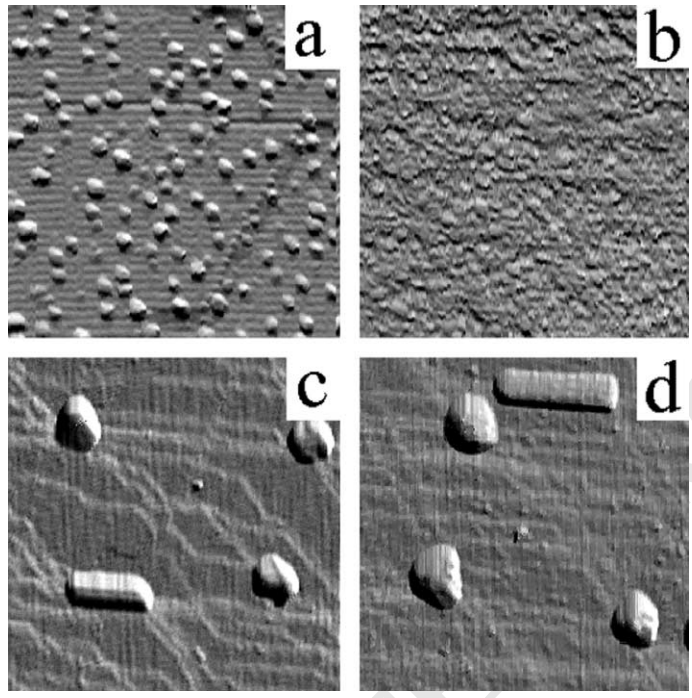

Fig. 2. Effects of CO adsorption on $Rh/TiO_2(110)$-(1×2) at two different particle sizes: (a,b) 2 nm, (c,d) 10–12 nm. (a,c) Before CO adsorption. (b,d) After exposures to CO, (b) 10^{-1} mbar, 300 K; (d) 10 mbar, 400 K.

3.3. Migration of surface carbon formed in the dissociation of CO

In this section, we follow the formation of carbonaceous species produced by the dissociation of CO on Rh nanoparticles and its diffusion. The coke formation is one of the crucial issues connecting to several catalytic processes (hydrocarbon refinery, CO conversion, etc.). This process usually causes a significant deactivation of the catalysts, however, in certain cases this reaction represents the main route for the catalytic production of different carbonaceous species, as for example fullerenes. In this case we utilized the advantage of STM namely that a chemical identification of the materials can be achieved by their characteristic structural properties. This has been generally used in the differentiation between the support and the deposited metals. The 2D model catalysts supporting metal clusters in large spatial separation provide excellent systems for studying the active sites in the formation of surface carbon and examining the diffusion properties of the different carbon forms.

Fig. 3(a) and (c) shows the surface textures of $Rh/TiO_2(110)$-(1×2) model catalysts grown by the "seeding + growing" method in two different image sizes of 200×200 and 400×400 nm, respectively. The Rh nanoparticles exhibit two characteristic forms: (i) hexagonal outline crystallites with (111) terraces; (ii) strongly elongated crystallites oriented in the [001] direction of the support. These surfaces were exposed to CO in the following experiments.

Fig. 3b depicts an STM image for Rh/TiO_2 following the CO exposure (10 mbar, 2 min) at 500 K. As appears, the original metal particles are practically unaltered, at the same time, however, new nanoparticles are formed with more or less characteristic size (15–20 nm) and coin-like shape. On the lower part of the image, two elongated Rh particles can be seen, on the upper part of the image two hexagonal Rh particles are detectable. These latter ones support adparticles on their top faces, the elongated particles (especially the longer one) are circumvented by the carbon adparticles. Naturally, from this image alone, it is not possible to declare that the deposited carbon is formed on the perimeter of the

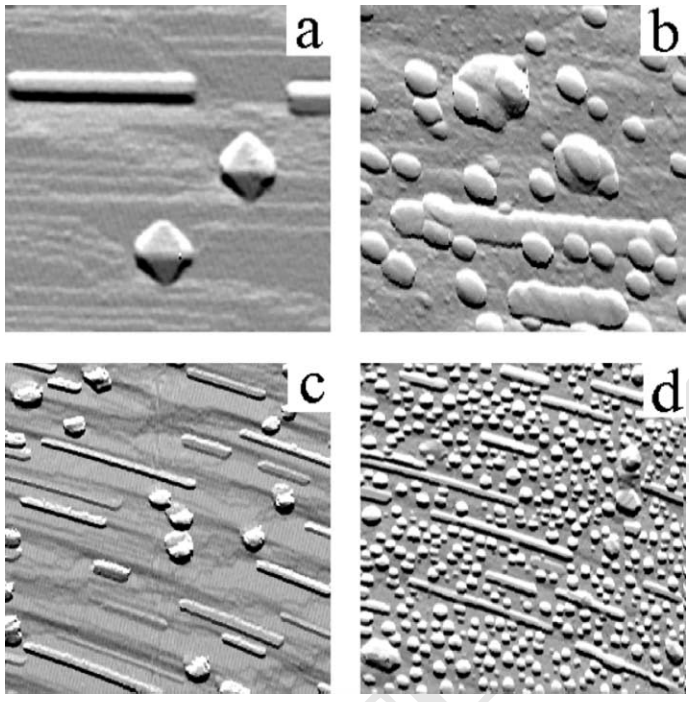

Fig. 3. Effects of thermal treatment of Rh-covered $TiO_2(110)(1 \times 2)$ surfaces in 10 mbar CO. (a,c) Before the treatment and after annealing in CO (b) at 500 K for 2 min; (d) at 500 K for 5 min followed by a short annealing at 900 K in UHV.

Rh nanoparticles; nevertheless, the morphology strongly suggests this conclusion. It also shows that the top sites of the round-shaped Rh particles bond the carbon clusters more strongly on their top face than the elongated ones. From the detailed study of the spatial distribution of these particles, it is possible to deduce some characteristics of the diffusion properties of the surface carbon [15]. A selected region of the same sample exposed to 10 mbar CO at 500 K for 5 min and annealed up to 900 K in UHV is depicted in Fig. 2d. It is clearly seen that the original Rh nanocrystallites remained practically unaltered, at the same time the intercrystallite regions are more or less uniformly covered by carbon particles of approximately 15 nm. It is remarkable that these new nanoparticles are definitely separated from the Rh crystallites on which they were formed. Particularly the elongated crystallites are free from the covering adparticles in this case. This fact suggests that the bonding of the carbon particles on the TiO_2 support is stronger than on the metal particles or on the perimeter sites of the oxide–metal interface. Although we could not perform dynamic STM measurements for an in situ investigation of carbon diffusion, from the behavior depicted above we can conclude that carbon is produced on metal particles and diffuses to the support.

4. Conclusions

Rh nanoparticles with desired size and average distance are prepared by the method consisting of two subsequent steps called as “seeding + growing”. The range of the particle size obtained is between 2 and 20 nm and the particle-neighbor distance can be easily tuned in the range of 5–100 nm. The simplicity of the method promises a wide-ranging application possibility for model studies in the field of heterogeneous catalysis. It is demonstrated that the reactivity of nanoparticles is primarily determined by their size in processes involving CO adsorption and reaction. The carbon formed on Rh nanoparticles diffuses onto $TiO_2(110)$ at and above 500 K, which can be readily followed by STM.

Acknowledgements

The authors gratefully acknowledge the support of the Hungarian Scientific Research Found through T-29952 and T-32040 projects.

References

[1] P.L.J. Gunter, J.W. Niemantsverdriet, F.H. Riberio, G.A. Somorjai, Catal. Rev. 39 (1997) 77.
[2] S.E. Aaron, R. Günther, L. Guczi, G.A. Somorjai, J. Phys. Chem. B 101 (1997) 9973.
[3] S.R. Foltyn, in: D.A. Payne, J.C. Bravman (Eds.), Laser Ablation for Materials Synthesis. Mater. Res. Soc. Symp. Proc., vol. 191, 1990, p. 205.
[4] Z. Pászti, G. Pető, Z.E. Horváth, A. Karacs, L. Guczi, J. Phys. Chem. B 101 (1997) 2109.
[5] F. Cerrina, C. Marrian, Mater. Res. Bull. 21 (1996) 56.
[6] K. Wong, S. Johansson, B. Kasemo, Faraday Discuss. 105 (1996) 237.
[7] P.B. Fischer, S.Y. Chou, Appl. Phys. Lett. 62 (1993) 2989.
[8] P.W. Jacobs, F.H. Riberio, G.A. Somorjai, S. Wind, J. Catal. Lett. 37 (1996) 131.
[9] P.W. Jacobs, S. Wind, F.H. Riberio, G.A. Somorjai, Surf. Sci. 372 (1997) L249.
[10] G.A. Somorjai, Appl. Surf. Sci. 121 (1998) 1.
[11] M. Frank, S. Andersson, J. Libuda, S. Stempel, A. Sandell, B. Brena, A. Giertz, P.A. Brühwiler, M. Bäumer, N. Mårtensson, H.-J. Freund, Chem. Phys. Letter 279 (1997) 92.
[12] A. Berkó, G. Klivényi, F. Solymosi, J. Catal. 182 (1999) 511.
[13] A. Berkó, G. Ménesi, F. Solymosi, Surf. Sci. 372 (1997) 202.
[14] A. Berkó, F. Solymosi, Surf. Sci. 400 (1998) 281.
[15] A. Berkó, T. Bíró, F. Solymosi, J. Phys. Chem. B 104 (2000) 2506.
[16] G.E. Poirier, B.K. Hance, J.M. White, J. Chem. Phys. 97 (1993) 5965.
[17] A. Berkó, F. Solymosi, Langmuir 12 (1996) 1257.
[18] S. Fisher, A.W. Munzk, K.D. Schierbaum, W. Göpel, Surf. Sci. 337 (1995) 17.
[19] I.D. Cocks, Q. Guo, R. Patel, E.M. Williams, E. Roman, J.L. Desegovia, Surf. Sci. 377 (1997) 135.
[20] Q. Guo, I.D. Cocks, E.M. Williams, Phys. Rev. Lett. 77 (18) (1996) 3851.
[21] R.E. Tanner, M.R. Castell, G.A.D. Briggs, Surf. Sci. 412–413 (1998) 672.
[22] R.A. Benett, P. Stone, N.J. Price, M. Bowker, Phys. Rev. Lett. 82 (1999) 3831.
[23] H.F.J. Van't Blick, J.B.A.D. Van Zon, T. Huizinga, J.C. Vis, D.C. Königsberger, R.J. Prins, J. Phys. Chem. 87 (1983) 2264.
[24] H.F.J. Van't Blick, J.B.A.D. Van Zon, T. Huizinga, J.C. Vis, D.C. Königsberger, R.J. Prins, J. Am. Chem. Soc. 107 (1985) 3139.
[25] F. Solymosi, M. Pásztor, J. Phys. Chem. 89 (1985) 4789.
[26] F. Solymosi, M. Pásztor, J. Phys. Chem. 90 (1986) 5312.
[27] A. Berkó, G. Ménesi, F. Solymosi, J. Phys. Chem. 100 (1996) 17732.
[28] J. Evans, B.E. Hayden, M.A. Newton, Surf. Sci. 462 (2000) 169.
[29] M. Frank, S. Andersson, J. Libuda, S. Stempel, A. Sandell, B. Brena, P.A. Brühwiler, M. Bäumer, N. Mårtensson, H.-J. Freund, Chem. Phys. Lett. 279 (1997) 92.